

# Chitosan/AuNPs Modified Graphene Electrochemical Sensor for Label-Free Human Chorionic Gonadotropin Detection

Sofia Teixeira, Nadia S. Ferreira, Robert Steven Conlan, O. J. Guy, and M. Goreti F. Sales

**Abstract:** A new immunosensor is presented for human chorionic gonadotropin (hCG), made by electrodeposition of gold nanoparticles over graphene screen-printed electrode (SPE). High selectivity was observed in blank urine and successful detection of hCG was also achieved in spiked samples of real urine bound to CS via its Fc-terminal. The assembly was controlled by electrochemical Impedance Spectroscopy (EIS) detection capability, simplicity of fabrication, low-cost, and followed by Fourier Transformed Infrared (FTIR). The hCG-immunosensor displayed linear response against the logarithm-hCG concentration for 0.1–25 ng/mL with limit of detection of 0.016 ng/mL. High selectivity was observed in blank urine and successful detection of hCG was also achieved in spiked samples of real urine bound to CS via its Fc-terminal. The assembly was controlled by electrochemical Impedance Spectroscopy (EIS) detection capability, simplicity of fabrication, low-cost, and followed by Fourier Transformed Infrared (FTIR). The hCG-immunosensor displayed linear response

**Keywords:** Immunosensor · Screen-printed electrode · Graphene · Antibody · Chitosan · Human chorionic gonadotropin

## 1 Introduction

Immunosensors make use of antigen-antibody interactions [1, 2] to detect a wide range of analytes which are of great interest in medical diagnostics, environmental analysis, and forensic medicine [3, 4], including pathogens [5], drugs [6], bacteria [7], toxins [8], and biomarkers [9]. Overall, immunosensors employ the same chemical approach of earliest immunoassays, but offer quicker and simpler analytical procedures that may be conducted at the point-of-care [10]. Immunosensors use an antibody immobilized as a transducer. Antigen-antibody binding event result in electrical or optical changes.

The interaction of the antigen with the immobilized antibody may be monitored using several detection methods. In this context, electrochemical immunosensors are increasingly being used for biosensing applications [11]. Electrochemical impedance spectroscopy (EIS) is an electrochemical technique, facilitating label-free detection [12, 13], thereby yielding significant advantages in terms of simplicity and rapidity compared to conventional immunosensing processes.

The immobilization of an antibody on the transducer element is a crucial step in the preparation of immunosensors [14, 15]. Physical adsorption is the simplest immobilization method, but it suffers from random antibody orientation and poor reproducibility [16–18]. Approximately 90 % of the antibodies are in an inactive orientation, due to steric blocking of antigen binding sites on these antibodies [12, 19]. More-stable and reproducible antibody binding is achieved by covalent attachment, but this attachment must ensure that antigen binding sites are kept free [20]. For this purpose, antibody coupling to protein G/A has been used [21].

An alternative (simple and effective) method for Ab attachment uses chemical activation of the carboxylic groups at the Fc terminal of the antibody and subsequent covalent binding to the physical support [21, 22]. Although the antibodies may suffer from cross-linking by this process, the sensitivity and the reproducibility of such immunosensors are both enhanced when compared to random adsorption [21, 22] and the simplicity of the overall process dramatically improves when compared to other oriented-binding approaches. Such Ab modification requires subsequent binding to a transducing support carrying an amine layer.

Chitosan (CS) is a biocompatible natural polymeric material displaying excellent film forming and adhesion ability [23], and thereby may act as an excellent amine surface for Ab binding. The solubility of CS is limited but it may be achieved by ensuring acidic conditions leading

to the protonation of the multiple amine groups in the material ( $pK_a$  of 6.3) [24, 25]. Moreover, the deposition of CS films can be performed by using simple electrochemical approach [25–27]: at a constant electrode potential, protons are consumed at the cathode, resulting in a pH gradient being established in the vicinity of the cathode surface and yielding a stable and reproducible CS film. The limited electrical properties of this film are countered by including highly conductive and biocompatible nanomaterials, such as gold nanoparticles (AuNPs) within the CS film [27].

The electrical properties of the transducing material to which the CS film is bound are also of major relevance in electrical immunosensing. The most widely employed electrode material has been gold, but carbon-based nanostructures are now gaining increasing interest. Different carbon nanostructures, with different inherent electrical properties have been employed in this context, mostly carbon nanotubes (CNTs) [28, 29] and more recently (since 2005) graphene [30]. Graphene displays a combination of interesting properties, such large surface area, high electrical conductivity and biocompatibility [31–38]. Heterogeneous electron transfer (the transfer of electrons between graphene and molecule in solution, necessary for the oxidation/reduction of said molecule) occurs at the edges or at defects in the graphene basal plane [39]. Additional defects are introduced by functionalizing graphene materials, a necessary procedure for the antibody attachment to graphene, also inducing electron transfer. Overall, graphene is a suitable electrical nanomaterial for electrode support in immunosensing, but it is mostly employed as a composite material.

Thus, this paper proposes a new approach for immunosensing using a combination of electrodeposition of CS and AuNPs on a graphene support and subsequent binding of activated antibodies to this nanocomposite film. This combination was used to follow the human chorionic gonadotropin (hCG) in urine, a 37 kDa glycoprotein hormone, secreted by the trophoblastic cells of placenta [40], acting as an important diagnostic marker of early pregnancy. In healthy human serum and urine, the concentration of hCG is extremely low. The increased level of hCG in serum and urine is associated with the trophoblastic cancer and many diseases related to pregnancy [41]. Levels can first be detected by a blood test about 11 days after conception and about 12–14 days after conception by a urine test. In general, the hCG levels double every 72 hours, reaching its peak in the first ~12 weeks of pregnancy (~288 000 mIU/mL or ~58 mg/mL) and then will decline and level off for the remainder of the pregnancy. Although there is no single “normal” hCG level in early pregnancy and there is a very wide range of hCG values as pregnancy progresses, a minimum of 5 mIU/mL hCG (or 1 ng/mL) is expected within the 3<sup>rd</sup> week of pregnancy. The levels of hCG may also be altered/increased in the course of cancer diseases [41].

Conventional methods for determining hCG are immunoradiometric assays (IRMA) and enzyme-linked immu-

nosorbent assays (ELISA) [42]. IRMA is extremely sensitive, but involves radiation hazards, complicated washing procedures and is expensive, while the ELISA is less sensitive but time-consuming. Several immunosensing devices for hCG have been reported in the literature so far [43–47], including different compositions and composite combinations, different detection methods and different strategies to enhance the number of free antigen-binding sites. Overall, the main interest in point-of-care context is to develop a simple and low cost procedure for the routine determination of hCG, where the complexity by which the biosensor is assembled is of outmost importance, mostly considering that immunosensing devices are of single use.

Thus, this work tries to establish a simple procedure at the stage of biosensor development, employing label-free electrochemical impedimetric detection. All chemical modifications made to the graphene electrode in a commercial SPE have been optimized and characterized using EIS and FTIR. The analytical features of the final device have been evaluated in buffer and urine samples, and its applicability tested in real urine.

## 2. Experimental

### 2.1 Reagents and Solutions

All chemicals used were of analytical grade and water was mostly ultrapure grade. Potassium hexacyanoferrate III ( $K_3[Fe(CN)_6]$ ), potassium hexacyanoferrate II ( $K_4[Fe(CN)_6]$ ) trihydrate and magnesium chloride were obtained from Riedel-deHaen; CS, AuNPs (<100 nm, 99.9%); *N*-(3-dimethylaminopropyl)-*N*-ethylcarbodiimide hydrochloride (EDAC) and bovine serum albumin (BSA) were obtained from Sigma; acetic acid was obtained from Carlo Erba; *N*-hydroxysuccinimide (NHS) and creatinine were obtained from Fluka; Phosphate Buffered Saline (PBS) tablets were obtained from Amresco; hCG protein was purchased from Abcam (UK); anti-hCG antibody was supplied by Ig Innovations (affinity constant for hCG of  $2.9 \times 10^{10}$  1/*M*, where *M* is 0.03 nM); ammonium chloride and calcium chloride were obtained from Merck; sodium dihydrogen phosphate was obtained from Scharlau; potassium sulfate and sodium chloride were obtained from Panreac; and urea was obtained from Fragon.

Firstly, a 1% (v/v) acetic acid solution was prepared in deionised water. Chitosan was then added to obtain 0.1% (w/w) solution. Finally, AuNPs were also added (as bought from Sigma or else prepared from gold in 5–50 nm size) to obtain a 1% (v/v). PBS solution was prepared by dissolution of 1 tablet of PBS in 100 mL of deionised water. EDAC, NHS and antibody solutions were prepared in this buffer. Synthetic urine was prepared by mixing several individual solutions leading to a final composition of  $5 \times 10^{-6}$  M urea,  $5.3 \times 10^{-6}$  M creatinine,  $9.8 \times 10^{-7}$  M magnesium chloride,  $6.8 \times 10^{-7}$  M calcium chloride,  $3.2 \times 10^{-6}$  M sodium dihydrogen phosphate,  $3.3 \times 10^{-6}$  M ammonium chloride,  $3.9 \times 10^{-6}$  M potassium sulfate and

$6.5 \times 10^{-6}$  M sodium chloride. A redox probe solution was prepared in PBS buffer and had a concentration of 5.0 mmol/L of  $[\text{Fe}(\text{CN})_6]^{3-}$  and 5.0 mmol/L of  $[\text{Fe}(\text{CN})_6]^{4-}$ .

## 2.2 Apparatus

Electrochemical measurements were conducted with a potentiostat/galvanostat, Metrohm Autolab, PGSTAT302N, controlled by Nova software and equipped with a Frequency Response Analysis module. Graphene-SPEs were purchased from DropSens (DRP-110GPH) and were composed of a carbon counter electrode, an Ag pseudo-reference electrode, and a printed graphene working electrode ( $\varnothing = 4$  mm). Electrical characterization of SPEs was performed by connecting the SPEs to the potentiostat/galvanostat via a suitable switch box (DropSens).

FTIR measurements were performed using an infrared spectrometer from Thermo Scientific, Smart iTR, Nicolet iS10, coupled to an Attenuated Total Reflectance (ATR) accessory also from Thermo Scientific, equipped with a Germanium sample holder.

## 2.3 Procedures for Immunosensor Assembly

The chitosan (CS) film was obtained by electrodeposition of chitosan on the graphene-SPE surface using chronoamperometry (CA). The three-electrodes of the SPE were covered by a solution of 0.1 % of chitosan and 1 % of AuNPs. A potential of  $-2.5$  V was applied for 120 s.

A drop of activated antibody solution was then cast over the CS-AuNPs film on the working electrode, and incubated for 2 hours, at room temperature. The activated antibody solution had been pre-prepared, by incubating a 200 mg/mL antibody solution in 25 mmol/L EDAC and 50 mmol/L of NHS, for 2 hours, at room temperature. Following exposure of the working electrode to the activated antibody solution the working electrode was then thoroughly rinsed with PBS and incubated in BSA solution (0.5 mg/mL in PBS buffer) solution, for 30 minutes. The immunosensor was finally washed with PBS buffer and kept at  $4^\circ\text{C}$  before use.

## 2.4 Human Chorionic Gonadotropin Binding

hCG binding to the immobilized antibody was achieved by placing a drop of hCG solution on the immunosensor working electrode surface. Different concentrations of hCG solutions, ranging from 0.01 to 100 ng/mL, were prepared by dilution of the 250 ng/mL standard hCG solutions in PBS or synthetic urine. hCG was also detected in real urine samples from pregnant women. A period of 20 minutes was allowed for antigen/antibody binding. This was followed by PBS washing prior to redox probe EIS measurements.

## 2.5 Electrochemical Assays

CV and EIS assays were conducted in triplicate. CV measurements were conducted in 5.0 mmol/L of  $[\text{Fe}(\text{CN})_6]^{3-}$  and 5.0 mmol/L of  $[\text{Fe}(\text{CN})_6]^{4-}$ , prepared in PBS buffer, pH 7.4, using a potential scan from  $-0.7$  to  $+0.7$  V, at 50 mV/s. EIS assays were made using the same redox couple  $[\text{Fe}(\text{CN})_6]^{3-/4-}$  solution, at a standard potential of  $+0.10$  V, using a sinusoidal potential perturbation with amplitude of 100 mV and a frequency of 50 Hz, logarithmically distributed over a frequency range of 100 000–0.1 Hz. Impedance data was fitted to a  $R(RC)$  circuit, the simplified Randles circuit, using the Nova Software. This circuit included solution resistance ( $R_s$ ), double layer capacitor ( $C_{dl}$ ), and charge transfer resistance ( $R_{ct}$ ) components, where double-layer capacitance and charge-transfer resistance are in parallel [48].

The immunosensor response to varying hCG concentrations was assessed by EIS measurements. The hCG solutions ranged from 0.01 to 100 ng/mL, and were prepared either in PBS buffer pH 7 or in synthetic urine. The LOD was the hCG concentration at which the calibration curve corresponded to a signal of 3 s, where s is the standard deviation of EIS blank signals (obtained in the absence of the hCG).

## 3 Results and Discussion

### 3.1 Immunosensor Assembly

The first surface modification step consisted of electrochemical oxidation of the graphene support. This oxidation produced a clean and reproducible surface, containing several hydroxyl groups (Figure 1 A). Hydroxyl groups display a high electrostatic affinity to amine-based materials such as CS, due to inherent electrostatic interactions predominantly in hydrogen bonding.

The solution of CS and AuNPs was then electrodeposited over the oxidized graphene (Figure 1 B), yielding an amine-terminated layer. Deposition of CS, as a method for producing an amine surface was tested in several ways, from drop-casting to electrodeposition, with or without AuNPs. Some of the conditions tested yielded a degraded graphene surface, with graphene flakes detaching into solution and destroying the working area of the SPE. Optimised conditions led to a stable working electrode area modified with CS and AuNPs.

Following deposition of the CS/AuNP layer, the Ab is attached to the CS via its  $\text{NH}_2$  groups (Figure 1 C). This was achieved by activating the  $-\text{COOH}$  groups at the Fc terminal of the antibody to orientate it on the sensor platform, with the highest probability of having all binding sites accessible for antigen binding. This activation was made using conventional EDAC/NHS chemistry: (1) reaction of  $-\text{COOH}$  with EDAC forms a *O*-acylisourea intermediate that subsequently reacted with NHS to produce a more stable active ester; (2) this ester undergoes nucleophilic substitution with any amine group on the

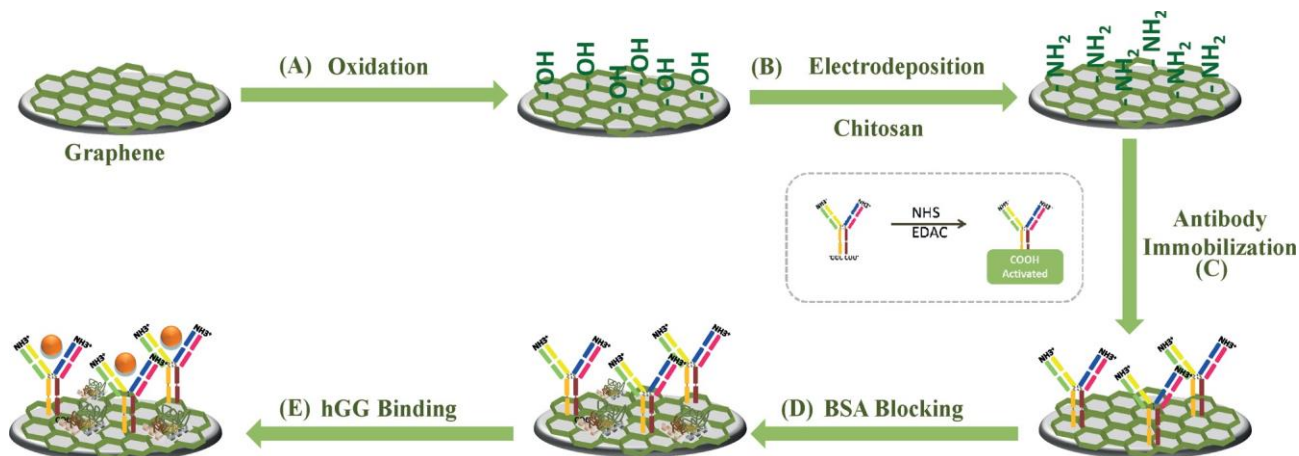


Fig. 1. Schematic illustration of the immunosensor assembly.

surface, resulting in the formation of an amide bond and subsequent covalent linkage of the antibody to the biosensor [49]. Any unbound protein was removed from the surface by thorough washing with PBS buffer.

The final stage of the sensor assembly was devoted to blocking any free  $\text{NH}_2$  binding sites on the surface that could participate in non-specific binding. This was done by adding BSA (Figure 1 D), a common protein in biological fluids. BSA interacts with any available protein binding site, blocking these binding sites to side-proteins in real samples. This reaction also contributed to deactivating carboxylic positions, thereby eliminating side-responses from the immunosensor.

The binding event between hCG and the immunosensor antibody is the final stage of the device development (Figure 1 E). This event is detected electrochemically. A mathematical relation between the analyte concentration and the obtained electrical signal was derived.

### 3.2 Electrochemical Follow-Up of the Immunosensor

Chemical modifications taking place at the graphene surface were followed by EIS (Figure 2), by monitoring the changes in the electron transfer properties of the iron redox probe [50]. EIS data was recorded in the form of Nyquist plot, showing the frequency response of the elec-

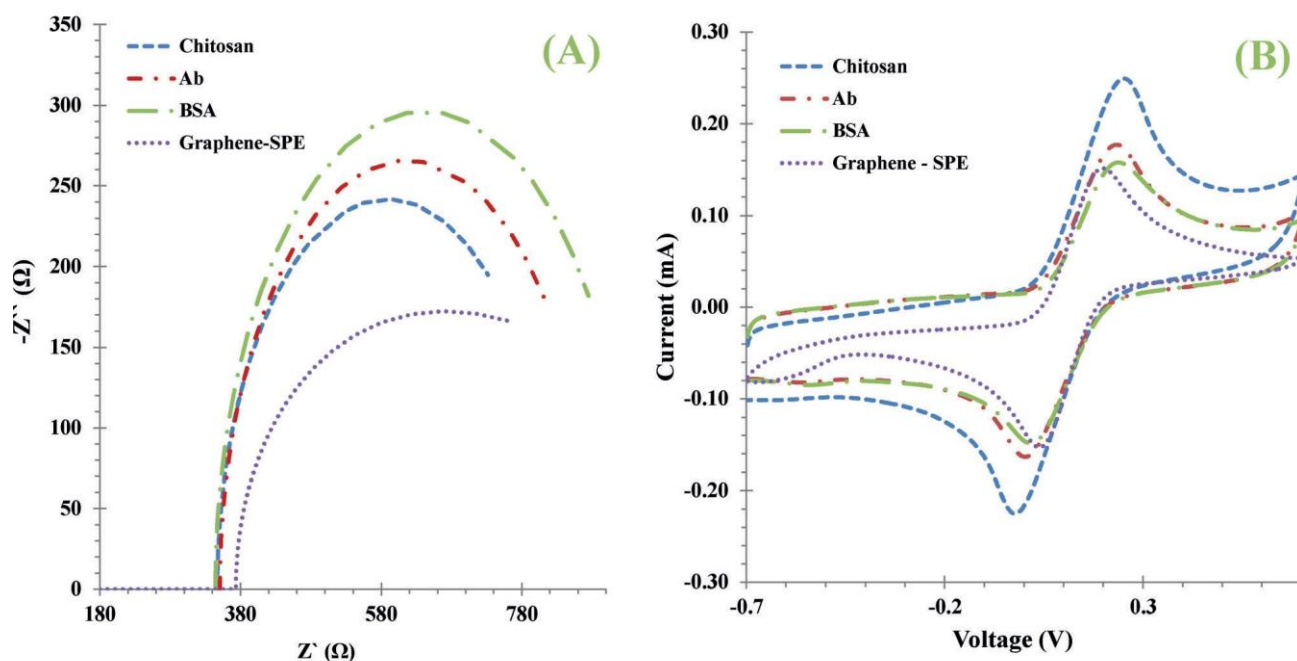


Fig. 2. EIS spectra of each stage of the assembly of the immunosensor (A) and CV data taken at each stage (B). (A) Nyquist plots of BSA/anti-hCG/CS/graphene-SPE sensor, obtained in 5.0 mM  $[\text{Fe}(\text{CN})_6]^{3-/4-}$  PBS buffer pH 7.4. (B) CV record after modification of chitosan/AuNPs/graphene-SPE with antibody and BSA.

trode/electrolyte system and an area plot of the imaginary component ( $-Z$ ) of the impedance against the real component ( $Z$ ). The  $R_{ct}$  at the electrode surface is given by the semicircle diameter of obtained in Nyquist plot and was used to define the interface properties of the electrode.

The nonmodified graphene-SPEs showed a very small semicircle at the Nyquist plot, indicating the presence of a very fast electron-transfer process on the graphene support (Figure 2 A). Subsequent deposition of a CS/AuNPs film contributed to an increase in the  $R_{ct}$ , thus acting as a barrier to the electron transfer of the redox probe. This increase is small but consistent with the presence of a polymeric material that has a small fraction of protonated amine functions (bearing the opposite charge to that of the redox probe) and AuNPs included in its matrix. Subsequent antibody and BSA binding, both protein materials, generated an additional increase in the  $R_{ct}$ , indicating as an additional barrier to electron transfer pro-

cesses. All CV assays supported the results of EIS studies (Figure 2 B), with decreased current peaks after protein binding and an increase in the peak-to-peak potential separation.

### 3.3 Qualitative Analysis of the Immunosensor Surface

Figure 3 shows the FTIR spectra of the different stages of assembly of the immunosensor on graphene-SPEs. The bare graphene spectra displayed very small intensity and no significant band/peak was observed (pink line).

The presence of CS on graphene after electrodeposition is shown by the adsorption peak centred at  $3362\text{ cm}^{-1}$  (blue line), corresponding most probably to a combination of both O–H and N–H stretching and intermolecular hydrogen bonding within CS molecules [51–53]. Although O–H stretching is expected to lead to a very intense absorption peak, the amount of CS on the surface is probably too small for this observation. The CS

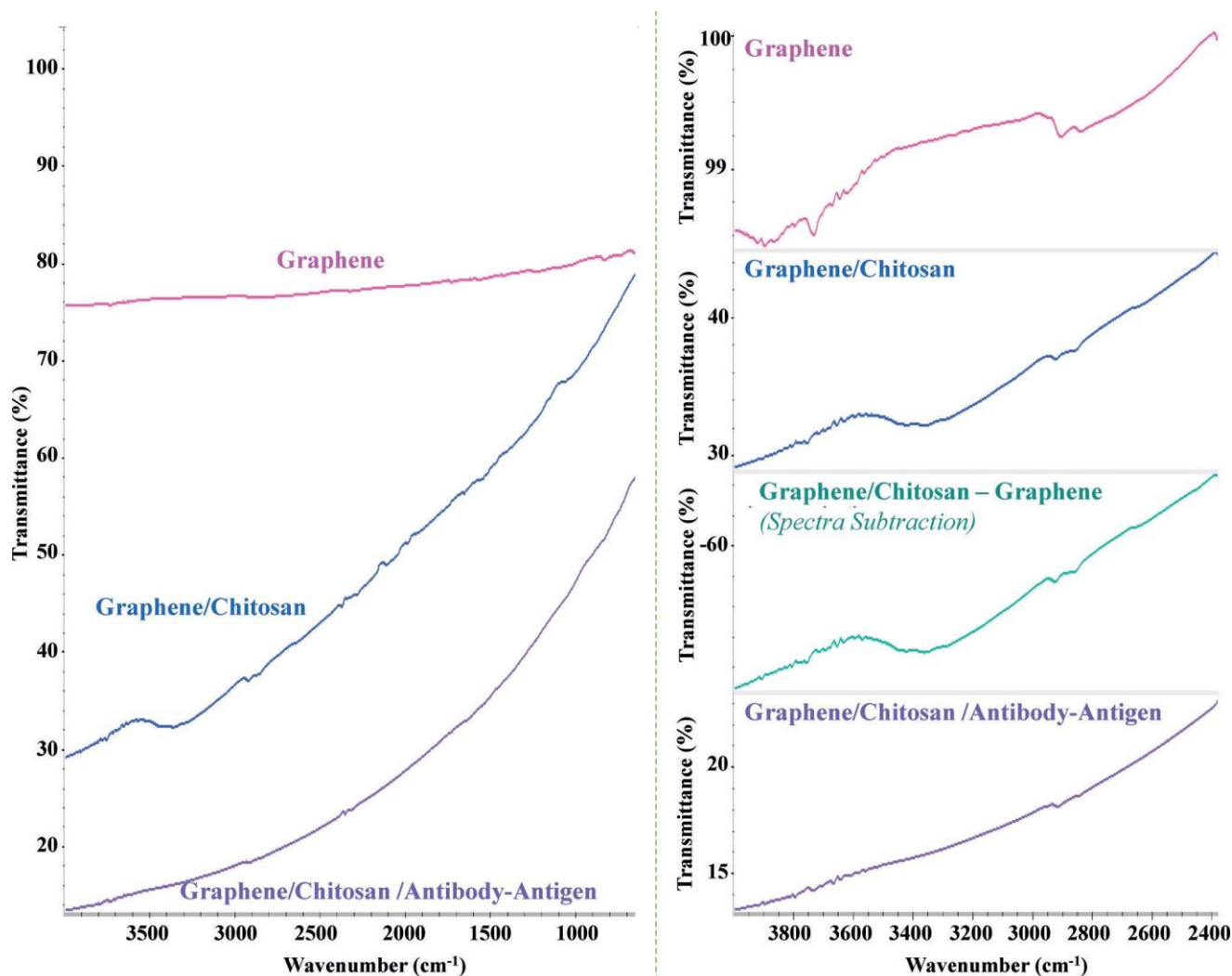


Fig. 3. FTIR spectra of the graphene-SPEs and graphene modified with CS and antibody/antigen (spectra on the right correspond to a smaller range of wavenumber, focusing the transmittance range of interest).



film on graphene also shows two small peaks lying within 2850–2950  $\text{cm}^{-1}$  that corresponded to C–H stretching.

The presence of antigen and antibody on graphene/CS contributes to additional light absorption. No peak is evidenced on the corresponding spectra (purple), which is probably a consequence of the low transmittance observed, being close to saturation (almost no light is transmitted). Overall, this spectra confirms the presence of an additional layer over CS.

### 3.4 Analytical Performance

Figure 4 A shows the Nyquist plots of the immunosensor as a function of increasing hCG concentrations. The concentration range of hCG used for calibration ranged from 0.1 to 25 ng/mL, with all solutions prepared in PBS. The corresponding calibration curve was plotted as  $R_{ct}$  (extracted from the Nyquist plots) against the logarithm of the hCG concentration (Inset of Figure 4 A). Overall, the  $R_{ct}$  increased logarithmically over the tested concentration range. The average slope of the  $R_{ct}$  versus  $\log[\text{hCG, ng/mL}]$  was 0.129 kW/decade hCG with an  $R^2$  correlation coefficient of 0.95. LOD was 0.016 ng/mL.

The analytical response of the immunosensor was considered irreversible, probably related to the high affinity between hCG and its antibody.

The sensor was always produced in one day, kept at 4  $^{\circ}\text{C}$  and analysed in the following day. Thus, it can be said that it was stable for 24 hours, but longer periods may be found when stored at 4  $^{\circ}\text{C}$  (as other immunosensors).

### 3.5 Selectivity of the Sensor

Sensor selectivity was assessed by evaluating the sensor response to the combined effect of any nonspecific compounds present in the samples analysed. This was done by calibrating the immunosensor-SPE in synthetic urine [54] and assessing any changes within the analytical performance of the device. Figure 4 B shows the Nyquist plots obtained in this context. Unexpectedly, the performance of the device improved, showing a wider  $\log[\text{hCG}]$  response range and increased sensitivity. The linear response ranged from 0.1 to 5 ng/mL and the average slope was of 0.353 kW/decade.

Overall, the analytical performance of the immunosensor was unexpectedly enhanced. Although this may indicate interference in the electrical response of the immunosensor by changing the medium in which it was evaluated, the existence of a linear range in the response of the electrode suggested that a successful application of the device in real urine samples could be achieved.

### 3.6 Application to Urine Samples

The values of hCG in real urine samples were determined by EIS measurements after previous calibration of the device in real urine of non-pregnant women. The typical Nyquist plots obtained are shown in Figure 5, along with the corresponding calibration curve.

The device exhibited a linear logarithmic behaviour from 0.01 to 1 ng/mL, a narrower concentration range of linear logarithmic response than that observed with synthetic urine. The biggest difference in terms of analytical performance was reflected in the signal saturation at

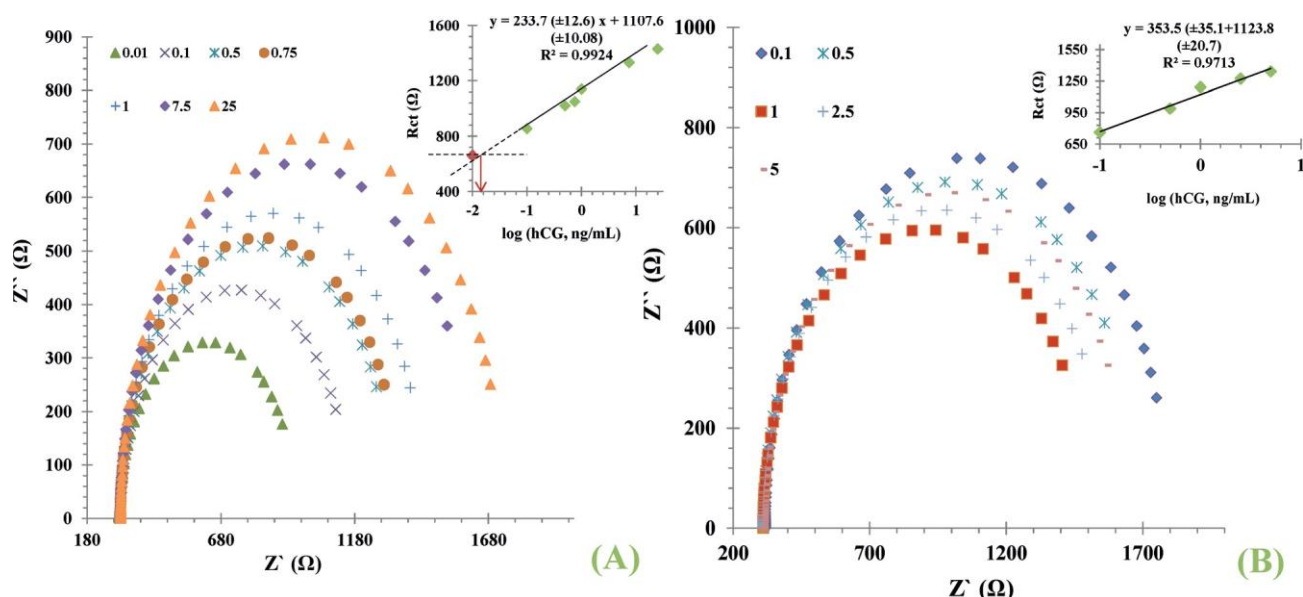


Fig. 4. Calibration curve of the immunosensor. (A) Nyquist plots of BSA/anti hCG/chitosan/graphene-SPE sensor, in 5.0 mM  $[\text{Fe}(\text{CN})_6]^{3-/4-}$  PBS buffer pH 7.4, previously incubated in increasing concentrations of hCG. (B) Nyquist plots of BSA/anti-hCG/chitosan/graphene-SPE sensor, in 5.0 mM  $[\text{Fe}(\text{CN})_6]^{3-/4-}$  synthetic urine pH 6.5, previously incubated in increasing concentrations of hCG.

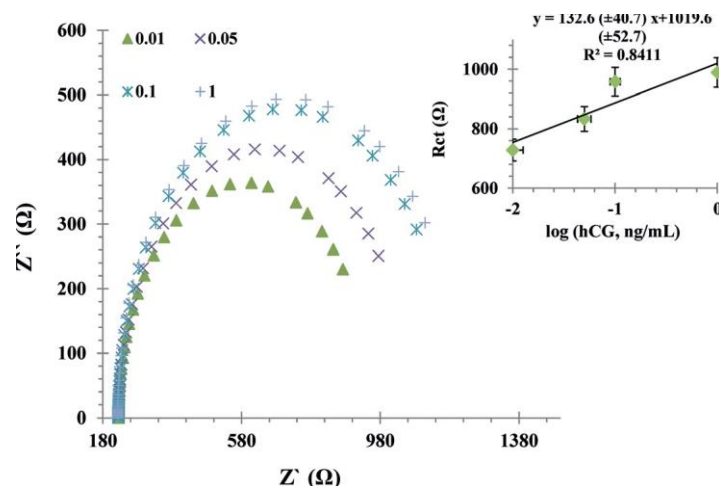


Fig. 5. Nyquist plots corresponding to the calibration of the immunosensor in real urine samples with hCG standards in ng/L. Inset: corresponding calibration curve, plotting  $\log(hCG)$  against  $R_{ct}$ .

lower hCG concentrations. Ever so, the format of the  $R_{ct}$  curve was similar to that of the calibration standards (Figure 5), suggesting that the system was operating well when using real urine samples.

A pristine but unused immunosensor was then used to analyse the urine of a pregnant woman, with a pregnancy of 3 to 5 weeks. The concentration of hCG obtained was 3.5 ng/mL (17.4 mIU/mL), which was in agreement with the pregnancy status.

#### 4 Conclusions

In summary, a new impedimetric biosensor for hCG determination in urine has been developed. A simple approach for generating a graphene-aminated surface to which an antibody binding with a suitable orientation for antigen binding is presented. The observed resistance to electron transfer increased linearly with increasing of  $\log(hCG)$  concentration.

The sensor response varied with the background medium used to calibrate the system and with the variations of blank immunosensor devices produced similarly. Once the immunosensor variability is eliminated by using relative impedance data (corrected against the blank, or zero concentration), the slopes become 0.371; 0.572 and 0.358, in buffer, synthetic urine and real urine. Therefore, only synthetic urine changed the typical calibration features. No plausible explanation for such differences in synthetic urine, apart from the eventual presence of some compound that may interact with the antibody directly (thereby changing its binding affinity for the antigen) and the pH differences between the matrices used in the calibration. However, if the background composition between samples and standards are tuned, no problem exists in the application of the immunosensor to the analysis of real samples, as proven by our results.

Overall, the sensor has been applied successfully to quantitatively detect hCG in the urine of pregnant

women, suggesting a successful application in point-of-care diagnostics in the near future.

#### Acknowledgements

This work is funded by the *European Social Fund (ESF)* through the *European Union's Convergence programme* administered by the *Welsh Government, Knowledge Economy Skills Scholarships (KESS)*, *EPSRC Project: EP/I00193X/1*. The authors would also like to acknowledge *IG innovations* for supplying the anti-hCG antibodies.

#### References

- [1] B. Kurtinaitiene, D. Ambrozaite, V. Laurinavicius, A. Ramanaviciene, A. Ramanavicius, *Biosens. Bioelectron.* 2008, 23(10), 1547–1554.
- [2] A. Ramanavicius, N. Kurilcik, S. Jursenas, A. Finkelsteinas, A. Ramanaviciene, *Biosens. Bioelectron.* 2007, 23(4), 499–505.
- [3] D. Grieshaber, R. MacKenzie, J. Vçrçs, E. Reimhult, *Sensors* 2008, 8, 1400–1458.
- [4] M. Suzuki, F. Ozawa, W. Sugimoto, S. Aso, *Anal. Bioanal. Chem.* 2002, 372(2), 301–304.
- [5] H. Vaisocherova, K. Mrkvova, M. Piliarik, P. Jinoch, M. Steinbachova, J. Homola, *Biosens. Bioelectron.* 2007, 22(6), 1020–1026.
- [6] G. Conneely, M. Aherne, H. Lu, G. G. Guilbault, *Anal. Chim. Acta* 2007, 583(1), 153–160.
- [7] E. Delibato, G. Volpe, D. Stangalini, De D. Medici, D. Moscone, G. Palleschi, *Anal. Lett.* 2006, 39.
- [8] D. Romanazzo, F. Ricci, S. Vesco, S. Piermarini, G. Volpe, D. Moscone, G. Palleschi, *JoVE* 2009, 32.
- [9] Y. Li, H. J. Lee, R. Corn, *Anal. Chem.* 2007, 79(3), 1082–1088.
- [10] J. Wang, *Biosens. Bioelectron.* 2006, 21(10), 1887–1892.
- [11] S. Sanchez, M. Roldan, S. Perez, E. Fabregas, *Anal.*

*Chem.*  
2008, 80(17), 6508–6514.



- [12] A. Kausaite-Minkstiniene, A. Ramanaviciene, J. Kirlyte, A. Ramanavicius, *Anal. Chem.* 2010, 82(15), 6401–6408.
- [13] 207–229.
- [14] J. M. Lee, H. K. Park, Y. Jung, J. K. Kim, S. O. Jung, Chung, *Anal. Chem.* 2007, 79(7), 2680–2687.
- [15] E. Dempsey, D. Diamond, A. Collier, *Biosens.* 2004, 20(2), 367–377.
- [16] Q. G.F. Xiong, *Expert. Rev. Proteomics* 2011, 8(4), 439–
- [17] C. A. McNulty, P. Lehours, F. Megraud, *Helicobacter* 16 Suppl 1, p. 10–18.
- [18] C. B. Moelans, R. A. de Weger, E. Van der Wall, P. J. iest, *Crit. Rev. Oncol./Hematol.* 2011, 80(3), 380–392.
- [19] J. E. Butler, L. N. W. R. Brown, K. S. Joshi, J. Rosenberg, E. W. Voss Jr, *Mol. Immunol.* 1993, 1165–1175.
- [20] J. Turkova, *J. Chromatogr. B, Biomed. Sci. Appl.* 1999, 1–2, 11–31.
- [21] N. Ferreira, M. Sales, *Biosens. Bioelectron.* 2014, 53, 193–199.
- [22] S. Teixeira, G. Burwell, A. Castaing, D. Gonzalez, Conlan, O. J. Guy, *Sens. Actuators B, Chem.* 2014, 190.
- [23] Y. Miao, S. N. Tan, *Anal. Chim. Acta* 2001, 437.
- [24] M. N. Kumar, R. A. A. Muzzarelli, C. Muzzarelli, H. Sashi-wa, A. J. Domb, *Chem. Rev.* 2004, 104(12), 6017–6084.
- [25] H. K. Solanki, D. D. Pawar, D. A. Shah, V. D. Prajapati, G. K. Jani, A. M. Mulla, P. M. Thakar, *BioMed. Res. Int.* 2013, 620719.
- [26] R. Fernandes, Li-Qun Wu, T. Chen, H. Yi, G. W. Rubloff, R. Ghodssi, W. E. Bentley, G. F. Payne, *Langmuir* 2003, 19.
- [27] A. Z. Rebecca, J. J. Park, G. W. Rubloff, M. J. Tarlov, *Elektrochim. Acta* 2006, 51.
- [28] J. Wu, Z. Fu, F. Yan, H. Ju, *TrAC – Trends Anal. Chem.* 2007, 26.
- [29] 2007, 26.
- [30] M. Pumera, A. Ambrosi, A. Bonanni, E. Chng, H. *TrAC – Trends Anal. Chem.* 2010, 29.
- [31] L. Yueming, T. Longhua, L. Jinghong, *Commun.* 2009, 11.
- [32] J. Li, S. Guo, Y. Zhai, E. Wang, *Anal. Chim. Acta* 649(2), 196–201.
- [33] X. Li, G. Zhang, X. Bai, X. Sun, X. Wang, E. Wang, *Nature Nanotechnol.* 2008, 3(9), 538–542.
- [34] Q. Wei, R. Li, B. Du, D. Wu, Y. Han, Y. Cai, Y. Xin, H. Li, M. Yang, *Sens. Actuators B, Chem.* 2011,
- [35] R. McCreery, *Chem. Rev.* 2008, 108(7), 2646–2687.
- [36] M. Li, R. Li, C. M. Li, N. Wu, *Frontiers Biosci.* 2011, 3, 1308–1331.
- [37] Y. Shao, J. Wang, H. Wu, J. Liu, I. A. Aksay, Y. Lin, *analysis* 2010, 22(10), 1027–1036.
- [38] T. Kuila, S. Bose, P. Khanra, A. K. Mishra, N. H. Kim, Lee, *Biosens. Bioelectron.* 2011, 26(12), 4637–4648.
- [39] P. Martin, *Mater. Today* 2011, 14, 7–8
- [40] U. H. Stenman, A. Tiitinen, H. Alfthan, L. Valmu, *Human Reprod., Update* 2006, 12(6), 769–784.
- [41] M. Aizawa, A. Morioka, S. Suzuki, Y. Nagamura, *Anal. Bio-chem.* 1979, 94(1), 22–28.
- [42] T. K. Lim, T. Matsunaga, *Biosens. Bioelectron.* 2001, 16, 1063.